Oxygen induced faceting of Cu(911)

Surface Science 715 (2022) 121933

Contents lists available at ScienceDirect

Surface Science

journal homepage: www.elsevier.com/locate/susc

Oxygen induced faceting of Cu(911)

Benjamin Hagman [*,a], Andreas Schaefer [b], Helen Edström [a], Kim von Allmen [a], Johan Gustafson [a]

[a] Synchrotron Radiation Research, Lund University,Box 118, Lund, 221 00, Sweden
[b] Department of Chemistry and Chemical Engineering and Competence Centre for Catalysis, Chalmers University of Technology, Gothenburg, 412 96, Sweden

ARTICLE INFO

Keywords:
SXRD
Copper
Faceting
Vicinal surface

ABSTRACT

The oxidation of copper is essential for several fields, such as corrosion, catalytic methanol synthesis, and CO_2 electroreduction. However, the understanding of the oxidation of copper under various conditions is not complete. Here, we study the oxidation of the vicinal Cu(911) surface by O_2 with *in-situ* Surface X-ray Diffraction. It was found that the surface facets to (410), (401), and (100) which are stable in the parameter range of T = 25–400 °C and $p = 10^{-10}$–10^{-5} mbar O_2. The (410) and (401) facets are present until the surface is further oxidized to Cu_2O, at 10^{-5} mbar and above. These results further the knowledge on the oxidation of copper and its surfaces, which may be of importance for a wide range of applications.

1. Introduction

The oxidation of copper-based systems is important for the understanding of the corrosion of the material itself, but also for other fields such as heterogeneous catalysis and electrocatalysis. For example, studies investigating the interaction of CO_2 and Cu have observed CO_2 to oxidize Cu, changing its chemical properties [1,2]. Additionally, under-coordinated Cu sites have been found to be important in CO_2 reduction [2–5]. Hence, understanding the behavior of under-coordinated Cu sites in the presence of an oxidative environment helps the understanding of CO_2 interaction with Cu.

Although comprehensive work has been done on copper oxidation for both closed packed surfaces and vicinal surfaces, there are still gaps to be filled [6,7]. For Cu(911), which has 4.5 atoms wide (100) terraces with (111) steps separating the terraces (see left side of Fig. 1), Scanning Tunneling Microscope (STM) studies have established that the surface facets into (410) and (401) (hereafter denoted {410}), with 3.5 atoms wide terraces separated with (110) steps (see right side of Fig. 1), at an oxygen coverage of 0.5 ML [7–9]. Cu(100) has been found to form a missing row reconstruction at an oxygen coverage of 0.5 ML [10], but the structure of the oxygen-covered (410) surface has been determined not to reconstruct [9,11]. However, the stability of these surfaces under different conditions is still not fully known.

In order to fill this knowledge gap, we have investigated the oxidation of Cu(911) with *in-situ* Surface X-ray Diffraction (SXRD). The surface structure was explored in the parameter space of T = 25-400 °C and $p = 10^{-10}$ (UHV)-10^{-4} mbar O_2. As expected, we observed the formation of (410) and (401) facets at moderate exposures. When the O_2 pressure reaches $> 10^{-5}$ mbar, an ordered Cu_2O oxide grows as the {410} facets disappear.

2. Methods

2.1. Sample preparation

The Cu(911) surface was cleaned by cycles of argon ion bombardment at 1 kV, 3 mA, and 1×10^{-5} mbar for 15 min and subsequent annealing to 700 K for 30 min. The surface was considered clean when Low-Energy Electron Diffraction (LEED) showed a sharp (1×1) pattern and/or the SXRD showed sharp Crystal Truncation Rods (CTRs).

2.2. SXRD Measurements

The experiments were done at beamlines p21.2 at PETRA III, DESY [12], and I07 at Diamond Light Source [13]. At p21 a non-commercial UHV chamber was used that could dose gases up to 1×10^{-3} mbar. The chamber was also equipped with sputtering capabilities and a Quadrupole Mass Spectrometers (QMS). At Diamond the existing setup in hutch EH2 was used and we complemented the SXRD measurements with LEED. At both beamlines a large stationary 2D detector was used and the data was acquired by rotating the sample around its surface normal. The photon energy was 70.5 keV and 20 keV at P21 and I07, respectively.

Two types of experiments were preformed. In the first experiment the

* Corresponding author.
E-mail address: benjamin.hagman@sljus.lu.se (B. Hagman).

https://doi.org/10.1016/j.susc.2021.121933
Received 24 July 2021; Received in revised form 20 August 2021; Accepted 28 August 2021
Available online 29 August 2021

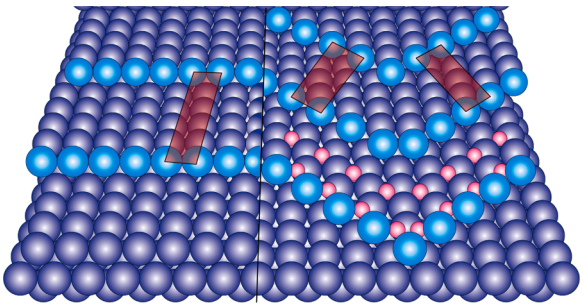

Fig. 1. A model of the Cu(911) surface (left) and a model of the faceted surface (right). The red rectangles indicate the unit cells of the (911), (410), and (401) surfaces. The turquoise balls show the step atoms, and the small red balls show the oxygen atoms on the (410) and (401) surface. (For interpretation of the references to colour in this figure legend, the reader is referred to the web version of this article.)

surface was exposed to 5.8×10^{-8} mbar O_2 at 400 °C and the oxidation was followed by measuring continuously around the (101) reflection and a super-structure rod. In the second experiment, the stability of the surface was explored by varying the temperature at a fixed O_2 pressure, for pressures of UHV to 1×10^{-4} mbar.

Positions in reciprocal space are denoted according to Cu(100) surface coordinates, where $|\mathbf{a}_1| = |\mathbf{a}_2| = a/\sqrt{2}$, $\mathbf{a}_1$ is parallel and $\mathbf{a}_2$ is perpendicular to the step edge, both parallel to the (100) plane. $\mathbf{a}_3$ is perpendicular to the (100) facet with length a. $a = 3.6$ Å is the bulk lattice parameter of Cu [14]. This results in reciprocal basis vectors of length $|\mathbf{b}_1| = |\mathbf{b}_2| = 2.46$ Å^{-1} and $|\mathbf{b}_3| = 1.74$ Å^{-1}, all parallel to the corresponding real basis vectors.

A map of the reciprocal lattice of the Cu(911) surface can be seen in Fig. 2. For the (911) surface, the (011) and (0$\bar{1}$1) reflections end up at different Q_z position, while the (101) and ($\bar{1}$01) do not. This can be seen in Fig. 2(b) and (c) which are slices of the reciprocal space around the Q_x and Q_y axis, respectively.

As mentioned above, previous STM studies showed that the surface facets to (410) and (401) [7,8]. This would result in two slanting CRTs

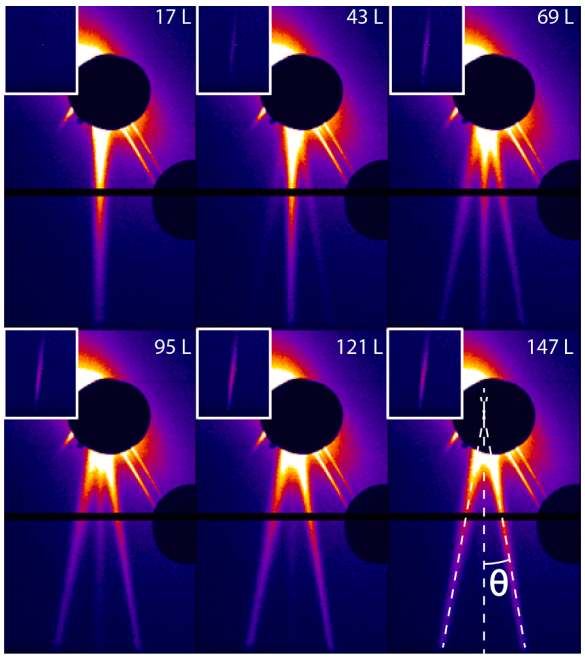

Fig. 3. Faceting of the Cu(911) surface with 5.8×10^{-8} mbar O_2 at 400 °C. The inserted images at the top-left corner are the super-structure rods for the faceted surface. The dashed white lines show the angle, $\theta \sim 10°$, between the facet CTRs and the Cu(911) CTR.

going through the Bragg reflections. This can be seen in Fig. 2(b) and (c) where the (410) and (401) CTRs are added around the (011), (0$\bar{1}$1), and (101) reflections. It should be noted that, from the point of view used in panel (b), the CTRs corresponding to (410) and (401) facets, respectively, will overlap and be seen as one. Additional to the CTRs, faceting into (410) and (401) will also give rise to super-structure rods. One of these super-structure rods is shown in Fig. 2(d).

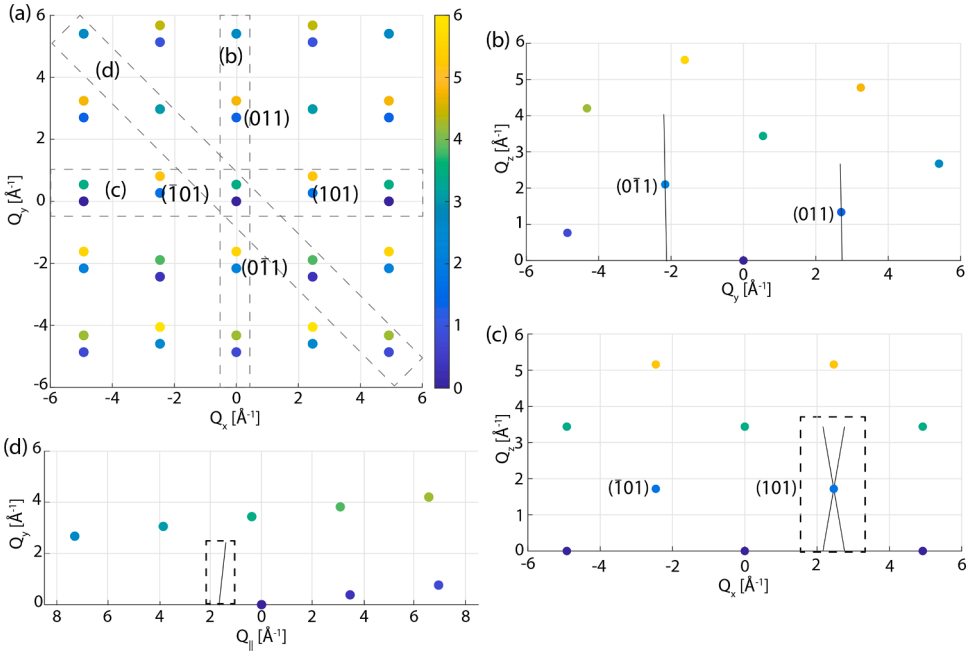

Fig. 2. Model of the reciprocal space of the Cu(911) crystal. (a) shows the reciprocal lattice of Cu(911) in the Q_x and Q_y plane, with the color gradient corresponding to Q_z. (b)-(d) show maps in the $Q_\parallel$, Q_z plane of the slices marked with dashed rectangles in (a). The lines show the expected directions of CTRs corresponding to (410) and (401) facets as seen in Fig. 3.

3. Results and discussion

Fig. 3 shows the development of the diffraction pattern around the (101) reflection (indicated with a dashed rectangle in Fig. 2c), as a function of oxygen dose, when the Cu(911) surface is exposed to 5.8 × 10^{-8} mbar O_2 at 400 °C. The images are created by summing the detector images of a rotation scan around the (101) reflection. Initially the CTR is vertical showing that the surface is un-faceted. However, as the oxygen exposure increases, two additional oblique CTRs appear. The new CTRs gradually take over and the (911) rods start to disappear as the oxygen exposure increases further. At 147 L the (911) rod has disappeared and only the two oblique CTRs are left. Hence, the surface facets to two new surface orientations.

Super-structure rods also appear as the surface is exposed to oxygen. This can be seen in the insets for each measurement in Fig. 3 (region in reciprocal space is indicated in 2 d with a dashed rectangle). Because the super-structure rods appear with the two new CTRs they should correspond to the faceted surface. The distance between the two rods is 1.7 $Å^{-1}$, corresponding to a real-space distance of 7.4 Å. This is close to the distance of 7.2 Å between the steps on the Cu(410) surface, showing that the super-structure rods correspond to the step periodicity of the surface. It should be noted that no super-structure rod was observed on the clean surface.

As the facet CTRs approximately lie in the same plane as the Ewald sphere, the direct detector images can be used to determine, to a close approximation, the angle between the facet CTRs and the (911) CTR. This is confirmed by transferring the images to positions in reciprocal space, see supporting information, which showed no significant difference. From the detector images in Fig. 3, the angle of the CTRs measures to be ~ 10°. This is close to the expected value of 9.9° between (410) and (911), which confirms faceting into {410}.

The corresponding super-structure rods of the facets will also lie in the same direction in reciprocal space as the CTRs. However, due to the view point seen in the detector (see Fig. 2c) one observes a projection of the rod and hence the angle measured on the detector image will be smaller.

As mentioned in the introduction, the facet formation is in agreement with previous STM experiments showing that Cu(911) facet to (410) and (401) [7,8]. The STM study also concluded that the facet size is a function of the temperature and pressure, with increasing size with increasing temperature and decreasing pressure. This is also in agreement with the present study, as a temperature of 400 °C was needed to get distinct CTRs. In the STM study, (100) facets were observed to form to compensate for the shorter steps on the {410} facets as compared to (911). However, no CTRs were observed corresponding the a (100) facet. This is most likely because the size of the (100) facets is too small to give a detectable diffraction signal, and hence cannot be seen in the experiment.

In addition to Cu(911) also (16 1 1), (15 1 1), (11 1 1), (711), and (511) surfaces have been found to form {410} facets upon oxidation [15–18]. The consequence is that these surfaces containing the more closed-packed (111) steps will instead form the more open (110) steps. This illustrates the importance of (110) steps, and (410) surface in particular, in the presence of oxygen. As (410) does not reconstruct, as Cu(100) does, one should not expect to find the missing row reconstruction on vicinal surfaces.

The stability of the surface was explored, by changing the conditions in the range of UHV - 1 × 10^{-4} mbar and RT - 400 °C, as illustrated in Fig. 4. There were no significant changes in neither the CTRs nor the super-structure rods in the range of UHV - 1 × 10^{-6} mbar and RT - 400 °C, which shows that the surface is stable for the range. However, in the range of 1 × 10^{-5}-1 × 10^{-4} mbar, Bragg reflections corresponding to Cu_2O oxide appear together with the gradual disappearance of the facet CTRs. Fig. 5 shows the diffraction pattern at 10^{-4} mbar and 400 °C, in perfect agreement with the expected diffraction from a well-ordered Cu_2O film, indicated by the black circles. More details on the properties of this Cu_2O film will be published separately.

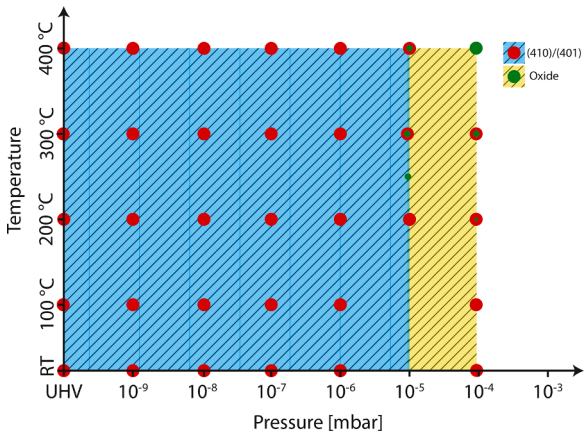

Fig. 4. The parameter space explored. The {410} facets are stable from UHV-1 × 10^{-6} mbar O_2, however at 1 × 10^{-5}-1 × 10^{-4} mbar oxide starts to grow. As the oxide grows the {410} facets disappear.

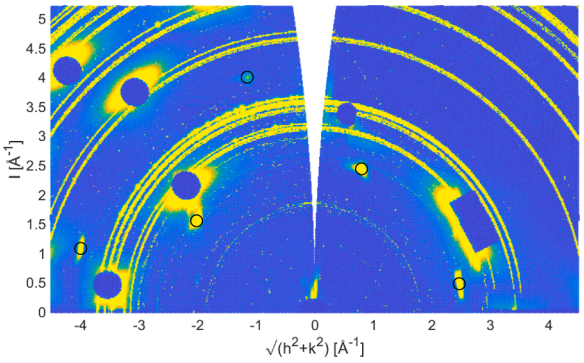

Fig. 5. Cu_2O formation. The Cu_2O Bragg reflections are indicated with black rings. As the Cu_2O appears the CTRs corresponding to {410} disappear.

On the Cu(100) surface the missing row reconstruction is blocking the dissociative adsorption of O_2, limiting the oxidation of the surface [19]. However, Cu(100) has been shown to form epitaxial oxide islands at O_2 pressures above ~ 10^{-4} mbar [20,21]. The formation of an oxide is most likely due to diffusion of the oxygen molecule to an area with excess Cu or surface defects [22,23]. This would suggest that stepped surfaces are more readily oxidized as there is a higher density of surface defects. Our impression is that this is indeed the case, although we lack data that are directly comparable. The difference is not as obvious as one might expect, which could suggest that the active defects are not the straight steps, but rather the ridge between the different facets.

There is a clear difference in the behavior of Cu(911) and Cu(100). For the Cu(100) surface there is a transformation of the $(2\sqrt{2} \times \sqrt{2})R45°$, missing row reconstruction, to a c(2 × 2) structure, with stochastically ordered Cu vacancies, at 200 °C [24]. However, on the (410) facets there is no such transformation, as there is no missing row reconstruction on the surface.

4. Conclusions

We have studied the oxidation of Cu(911) by O_2 using *in-situ* SXRD in the parameter range of $T = 25$–400 °C and $p = 10^{-8}$–10^{-4} mbar O_2. The results show that the surface rearranges to {410} facets, which are stable up to 10^{-5} mbar O_2, depending on temperature, where an ordered Cu_2O starts to grow.

As a result of the formation of {410} facets, there is a transformation of the (111) steps into (110) steps with the faceting. Hence, it is expected

that (110) steps should be present, rather than (111), in many reactions on the surface, such as CO_2 dissociation. This illustrates the importance of using (110) steps in such studies and for potential applications.

Although the initial oxidation of Cu(911) will produce {410} facets, they are not present as the oxide appears. This indicates that the {410} facets are not stable beyond the oxidation of the first Cu layer and that the oxide growth does not proceed on the {410} facets.

CRediT authorship contribution statement

Benjamin Hagman: Investigation, Data curation, Writing – original draft. **Andreas Schaefer:** Investigation, Writing – review & editing. **Helen Edström:** Investigation, Writing – review & editing. **Kim von Allmen:** Investigation, Writing – review & editing. **Johan Gustafson:** Project administration, Supervision, Investigation, Data curation, Writing – review & editing.

Declaration of Competing Interest

The authors declare that they have no known competing financial interests or personal relationships that could have appeared to influence the work reported in this paper.

Acknowledgments

We acknowledge DESY (Hamburg, Germany), a member of the Helmholtz Association HGF, for the provision of experimental facilities. Parts of this research were carried out at PETRA III and we would like to thank Dr. Ulrich Lienert, Dr.mont. Timo Mller, and Dr. Zoltan Hegeds for assistance in using beamline p21. Beamtime was allocated for proposal I-20190682 EC. The research leading to this result has been supported by the project CALIPSOplus under the Grant Agreement 730,872 from the EU Framework Programme for Research and Innovation HORIZON 2020. We acknowledge Diamond Light Source for time on I07 under proposal S122586-1. The authors thank the Swedish Research Council (No. 2014–04708_VR), the Swedish Foundation for Strategic Research, and the Knut and Alice Wallenberg Foundation (No: KAW 2015.0058) for financial support.

Supplementary material

Supplementary material associated with this article can be found, in the online version, at doi:10.1016/j.susc.2021.121933

References

[1] B. Eren, R.S. Weatherup, N. Liakakos, G.A. Somorjai, M. Salmeron, Dissociative carbon dioxide adsorption and morphological changes on cu(100) and cu(111) at ambient pressures, J. Am. Chem. Soc. 138 (2016) 8207–8211, https://doi.org/10.1021/jacs.6b04039.

[2] B. Hagman, A. Posada-Borbòn, A. Schaefer, M. Shipilin, C. Zhang, L.R. Merte, A. Hellman, E. Lundgren, H. Grönbeck, J. Gustafson, Steps control the dissociation of CO2 on cu(100), J. Am. Chem. Soc. 140 (2018) 129712979, https://doi.org/10.1021/jacs.8b07906.

[3] A.A.B. Padama, J.D. Ocon, H. Nakanishi, H. Kasai, Interaction of CO, o, and CO_2 with cu cluster supported on cu(111): a density functional theory study, J. Phys.: Condens. Matter 31 (2019) 415201, https://doi.org/10.1088/1361-648x/ab2b66.

[4] D. Kopa, B. Likozar, M. Hu, Catalysis of material surface defects: multiscale modeling of methanolsynthesis by CO_2 reduction on copper, Appl. Surf. Sci. 497 (2019) 143783, https://doi.org/10.1016/j.apsusc.2019.143783.

[5] C.-C. Chang, M.S. Ku, Role of high-index facet cu(711) surface in controlling the c2 selectivity for CO_2 reduction reaction - a DFT study, J. Phys. Chem. C 125 (2021) 10919–10925, https://doi.org/10.1021/acs.jpcc.1c00297.

[6] C. Gattinoni, A. Michaelides, Atomistic details of oxide surfaces and surface oxidation: the example of copper and its oxides, Surf. Sci. Rep. 70 (2015) 42447, https://doi.org/10.1016/j.surfrep.2015.07.001.

[7] N. Reinecke, E. Taglauer, The kinetics of oxygen-induced faceting of cu(115) and cu(119) surfaces, Surf. Sci. 454/ 456 (2000) 94–100, https://doi.org/10.1016/S0039-6028(00)00272-7.

[8] N. Reinecke, S. Reiter, S. Vetter, E. Taglauer, Steps, facets and nanostructures: investigations of cu(11n) surfaces, Appl. Phys. A 75 (2002) 1–10, https://doi.org/10.1007/s003390101049.

[9] D.C. Sheppard, G. S. Parkinson, A. Hentz, P.D. Quinn, M.A. Muoz-Mrquez, D. P. Woodruff, P. Bailey, T.C.Q. Noakes, Surface relaxation in cu(4 1 0)o: a medium energy ion scattering study, Surf. Sci. 604 (2010) 788–796, https://doi.org/10.1016/j.susc.2010.02.001.

[10] M. Kittel, M. Polcik, R. Terborg, J.-T. Hoeft, P. Baumgrtel, A.M. Bradshaw, R. L. Toomes, J.-H. Kang, D.P. Woodruff, M. Pascal, C.L.A. Lamont, E. Rotenberg, The structure of oxygen on cu(100) at low and high coverages, Surf. Sci. 470 (2001) 311–324, https://doi.org/10.1016/S0039-6028(00)00873-6.

[11] E. Vlieg, S.M. Driver, P. Goedtkindt, P.J. Knight, W. Liu, J. Ldecke, K.A.R. Mitchell, V. Murashov, I.K. Robinson, S.A. de Vries, D.P. Woodruff, 2002, Structure determination of Cu(410)O using X-ray diffraction and DFT calculationsSurf. Sci 516, 16–32, 10.1016/S0039-6028(02)02066-6.

[12] P21 Swedish Materials Science Beamline., https://www.photon-science.desy.de/facilities/petra_iii/beamlines/p21_swedish_materials_science/index_eng.html (Accessed 24 June 2021).

[13] C. Nicklin, T. Arnold, J. Rawle, A. Warne, Diamond beamline i07: a beamline for surface and interface diffraction, J. Synchrotron Rad. 23 (2016) 12451253, https://doi.org/10.1107/s1600577516009875.

[14] M.E. Straumanis, L.S. Yu, Lattice parameters, densities, expansion coefficients and perfection of structure of cu and of cuin α phase, Acta Cryst. A 25 (1969) 676–682, https://doi.org/10.1107/S0567739469001549.

[15] J.C. Boulliard, C. Cohen, J.L. Domange, A.V. Drigo, A. L'Hoir, J. Moulin, M. Sotto, Atomic displacements on stepped (16,1,1) copper structures: a channeling study, Phys. Rev. B 30 (1984) 2470–2486, https://doi.org/10.1103/PHYSREVB.30.2470.

[16] M. Sotto, Oxygen induced reconstruction of (h11) and (100) faces of copper, Surf. Sci. 260 (1992) 235–244, https://doi.org/10.1016/0039-6028(92)90037-7.

[17] D.A. Walko, I.K. Robinson, Structure of cu(115): clean surface and its oxygen-induced facets, Phys. Rev. B 59 (1999) 15446–15456, https://doi.org/10.1103/PhysRevB.59.15446.

[18] P.J. Knight, S.M. Driver, D.P. Woodruff, Scanning tunnelling microscopy investigation of the oxygen-induced faceting and "nano-faceting" of a vicinal copper surface, Surf. Sci. 376 (1997) 374–388, https://doi.org/10.1016/S0039-6028(96)01328-3.

[19] M. Alatalo, A. Puisto, H. Pitknen, A.S. Foster, K. Laasonen, Adsorption dynamics of o_2 on cu(100), Surf. Sci. 600 (2006) 1571578, https://doi.org/10.1016/j.susc.2005.11.058.

[20] J.C. Yang, M. Yeadon, B. Kolasa, J.M. Bibson, Oxygen surface diffusion in three-dimensional cu_2o growth on cu(001) thin films, Appl. Phys. Lett. 70 (1997) 3522–3524, https://doi.org/10.1063/1.119220.

[21] K. Lahtonen, M. Hirsimki, M. Lampimki, M. Valden, Oxygen adsorption-induced nanostructures and island formation on cu{100}: bridging the gap between the formation of surface confined oxygen chemisorption layer and oxide formation, J. Chem. Phys. 129 (2008) 124703, https://doi.org/10.1063/1.2980347.

[22] S. Jaatinen, J. Blomqvist, P. Salo, A. Puisto, M. Alatalo, M. Hirsimki, M. Ahonen, M. Valden, Adsorption and diffusion dynamics of atomic and molecular oxygen on reconstructed cu(100), Phys. Rev. B 75 (2007) 075402, https://doi.org/10.1103/PhysRevB.75.075402.

[23] M. Ahonen, M. Hirsimki, A. Puisto, S. Auvinen, M. Valden, M. Alatalo, Adsorption dynamics of o_2 on cu(100): the role of vacancies, steps and adatoms in dissociative chemisorption of o_2, Chem. Phys. Lett. 456 (2008) 211214, https://doi.org/10.1016/j.cplett.2008.03.039.

[24] H. Iddir, D.D. Fong, P. Zapol, P.H. Fuoss, L.A. Curtiss, G. W. Zhu, J.A. Eastman, Order-disorder phase transition of the cu(001) surface under equilibrium oxygen pressure, Phys. Rev. B 76 (2007), https://doi.org/10.1103/PhysRevB.76.241404.24140412414044